

MiR-126 on mice with coronary artery disease by targeting S1PR2

J.-L. FAN, L. ZHANG, X.-H. BO

Department of Cardiology, Taihe People's Hospital, Fuyang, China

Abstract. – OBJECTIVE: To screen the differentially expressed micro ribonucleic acids (miRNAs) in the serum of coronary atherosclerosis patients, and to investigate their possible mechanisms of action.

PATIENTS AND METHODS: The differentially expressed serum miRNAs were screened from 3 coronary artery disease (CAD) patients and 3 healthy controls using miRNA expression profiles, which were verified using low-throughput quantitative Reverse Transcription-Polymerase Chain Reaction (RT-qPCR) assay. 60 apolipoprotein E (ApoE)^{-/-} mice were divided into model group, agomir-126 group, agomir-control (con) group, and antagomir-126 group using a random number table. They were fed with high-fat diets (21% fat and 0.15% cholesterol) *ad libitum* for 15 weeks to establish the mouse model of CAD. Then, hematoxylin and eosin (HE) staining was applied to detect the impact of miR-126 expression level on the tissue morphology in the thoracic aortic region. The influences of miR-126 expression level on the secretion levels of tumor necrosis factor- α (TNF- α), interleukin-1 beta (IL-1 β), and IL-10 were determined via enzyme-linked immunosorbent assay (ELISA). Western blotting assay was performed to examine the effects of miR-126 expression level on the expression levels of nuclear factor-kappa B (NF- κ B) and vascular cell adhesion molecule-1 (VACM-1) in the tissues of the thoracic aortic region of the mice. The correlation between miR-126 expression level and sphingosine-1-phosphate receptor 2 (S1PR2) in the serum of CAD patients and animal models was analyzed by the Pearson correlation coefficient method. The targets of miR-126 were predicted using the bioinformatics method, and the direct targets were verified through investigations. Western blotting assay and ELISA were adopted to detect the impacts of miR-126 expression level on the expression and secretion levels of TNF- α , IL-1 β , and IL-10 in S1P + oxidized low-density lipoprotein (ox-LDL)-induced human umbilical vein endothelial cells (HUVECs). Lentivirus-small hairpin RNA (shRNA) was utilized to knock down the expression level of S1PR2 to determine whether miR-126 affected the increase in the inflammation level in S1P + ox-LDL-induced HUVECs by targeting S1PR2.

RESULTS: Compared with those in control group, 4 miRNAs (miR-126, miR-206, miR-4297,

and miR-3646) in the serum of CAD patients exhibited the most significant expression differences, which increased by 6.72, 7.11, 13.57, and 21.22 times, respectively. The verification results of low-throughput RT-qPCR assay indicated that there were remarkable changes in the expression levels of the 4 selected miRNAs with differential expressions in comparison with those in control group, displaying statistically significant differences ($p < 0.01$). The results of HE staining manifested that the coronary atherosclerotic plaques were reduced markedly in agomir-126 group, while notably more coronary atherosclerotic plaques were formed in the thoracic aortic region in antagomir-126 group. Meanwhile, the elevated expression level of miR-126 evidently lowered the expressions of serum TNF- α and IL-1 β , but significantly increased the expression of IL-10 in the mouse model of CAD. According to the analysis results of the Pearson correlation coefficient method, the miR-126 expression level was negatively correlated with S1PR2 expression level in the serum of both CAD patients and animal models ($r = -0.6123$, $r = -5.37$). It was shown in bioinformatics prediction and luciferase reporter gene assay that miR-126 negatively regulated the S1PR2 expression by targeting the 3' untranslated region (UTR) of S1PR2 messenger RNA (mRNA). In the *in vitro* inflammation model, the increased expression level of miR-126 could relieve the inflammation in cells induced by S1P + ox-LDL. Based on the results of both Western blotting assay and ELISA, the differences in the expression and secretion levels of TNF- α , IL-1 β , and IL-10, as well as the expression levels of signaling molecules of the NF- κ B signaling pathway, in the cells were not statistically significant among miR-126 mimic treatment group, sh-S1PR2 group, and miR-126 mimic + sh-S1PR2 group, indicating that miR-126 affects the inflammation level in HUVECs by targeting S1PR2.

CONCLUSIONS: MiR-126 represses the progression of coronary atherosclerosis in the mice by binding to S1PR2. The results of this research may propose a new mechanism of miR-126 in exerting its therapeutic effects and possess potential value for the treatment of CAD in the future.

Key Words:

MiR-126, S1PR2, Coronary atherosclerosis, Inflammation.

Introduction

Coronary artery disease (CAD), also known as coronary atherosclerosis, has relatively high morbidity and mortality rates and causes disastrous impacts on the social economy¹. It is manifested as coronary artery stenosis and remodeling, leading to ischemia and hypoxia of the myocardial tissues, and ultimately resulting in myocardial necrosis. The pathological mechanism of CAD, with stable angina, acute coronary syndrome, acute myocardial infarction, and sudden cardiac death as the clinical manifestations, is fairly complex and related to multiple factors².

From the perspective of pathology, CAD is mainly characterized by the formation of coronary atherosclerotic plaques, whose pathological process arises from vascular endothelial dysfunction, vascular tone dysregulation, and coronary vasoconstriction. In the advanced stage, low-density lipoprotein (LDL) can induce the endothelial cells to express the vascular adhesion molecules and intercellular adhesion molecules, and then promote the adhesion of monocytes, thus stimulating the formation of foam cells³. Subsequently, the proliferation of vascular smooth muscle cells causes vascular stenosis and remodeling, finally blocking the blood supply and triggering tissue ischemia. The rupture of plaques will lead to thrombosis, and the sudden occlusion of arterial lumen will ultimately give rise to acute coronary syndrome⁴.

Micro ribonucleic acids (miRNAs), a kind of double-stranded non-coding RNAs with small molecular weights, are crucial post-transcriptional gene regulators⁵, whose action mechanism is to repress the expression or induce the degradation of messenger RNAs (mRNAs) by binding to their 3' untranslated region (UTR)⁶. Currently, several studies have manifested that miRNAs play extremely important roles in the pathological process of cardiovascular diseases. In the case of atherosclerosis, for example, numerous miRNAs are involved in the direct and indirect modulation of such vital pathological processes as vascular endothelial dysfunction, abnormal lipid regulation, infiltration of inflammatory cells, and differentiation of vascular smooth muscle cells⁷⁻⁹. However, there are still limited investigations into the crucial roles of miRNAs in coronary atherosclerosis at present.

Therefore, this research aims to screen the differentially expressed miRNAs in the serum of coronary atherosclerosis patients. The targets of

the miRNAs were predicted using bioinformatics method, and the direct targets were verified through investigations. Later, functional verification was performed at the *in vitro* and *in vivo* levels, hoping to further understand the pathological process of coronary atherosclerosis and seek for a novel category of molecular markers and drug targets to facilitate the diagnosis and treatment of the disease.

Patients and Methods

Research Subjects

21 CAD patients confirmed by angiography were set as CAD group. Those suffering from cardiac function impairment, heart failure, acute myocardial infarction or unstable CAD were excluded. 30 healthy volunteers without CAD and other inflammatory diseases were enrolled as control group. In addition, the exclusion criteria of this research are as follows: patients with a medical history of leukopenia or thrombocytopenia, or those with other inflammatory diseases. This investigation was approved by the Moral and Ethical Committee of our hospital, and all the CAD patients and healthy volunteers signed the informed consent.

Screening of Differentially Expressed miRNAs via miRNA Expression Profiles

Total RNAs were extracted from the serum samples of the two groups of subjects and then quantified using the NanoDrop kit (Thermo Fisher Scientific, Waltham, MA, USA). Next, the integrity of the RNAs was evaluated by Bioanalyzer 2100 (Agilent, Santa Clara, CA, USA). In this research, Affymetrix 3' IVT Express kit and 100 ng of total RNA were applied to prepare complementary RNA (cRNA), which was hybridized on the Affymetrix PrimeView Human Array at 45°C for 16 h according to the user manual of GeneChip 3' Array (Affymetrix, Santa Clara, CA, USA). In addition, the array was processed on the Affymetrix FS-450 Fluidics Station, followed by washing, staining, and scanning using the Affymetrix GeneChip Scanner in accordance with the manufacturer's protocol. The raw data in the CEL files were imported into Partek Genomics Suite 6.6 software, and the probe sets were standardized by Robust Multi-array Average method. Finally, one-way analysis of variance was adopted to determine the significance of the differentially expressed genes, and *p*-values were corrected by FDR.

Quantitative Reverse Transcription-Polymerase Chain Reaction (RT-qPCR) Assay

RT and qPCR were employed to detect the expression of miR-126 in the serum samples and large cell lines, and the mRNA expression of sphingosine-1-phosphate receptor 2 (S1PR2) in human umbilical vein endothelial cells (HUVECs). The total RNA samples (500 ng) for reverse transcriptase reaction were divided into three parts, each of which was diluted at 1:10. Then, 3 μ L of total RNA was taken for PCR amplification. After that, 5% agarose gel electrophoresis was performed to verify the amplification level of target genes. LabWorks 4.0 image acquisition and analysis software were used for data quantification and processing. U6 was selected as the internal reference in this research, and the primers of miR-126 were purchased from ABM (Peterborough, Cambridge, Canada). The samples in every group were measured three times to obtain reliable data. In this research, the $2^{-\Delta\Delta Ct}$ method was adopted to analyze the changes in relative expressions of target genes, and the primer sequences utilized are shown in Table I.

Cell Culture and Experimental Scheme

The HUVECs and HEK293 cell line used in this research were purchased from the American Type Culture Collection (ATCC; Manassas, VA, USA). The cells were cultured in Dulbecco's Modified Eagle's Medium (DMEM) containing 10% fetal bovine serum (FBS) and 1% penicillin/streptomycin in an incubator with 5% CO₂ at 37°C. Before the investigation, all the inoculated cells were subjected to serum-free culture for 8 h and synchronization.

MiR-126 mimic (miR-126), miRNA control (miR-con), miR-126 inhibitor, small hairpin RNA (shRNA) targeting S1PR2 (sh-S1PR2), and shRNA control (sh-con) were purchased from Shanghai GenePharma Co., Ltd (Shanghai, China). The full-length S1PR2 sequence was cloned into

lentivirus plasmid pLenti6/V5-D-TOPO vector (Invitrogen, Carlsbad, CA, USA) to establish the recombinant plasmid of S1PR2, with empty plasmid as the control.

In the preliminary investigation, all the cells were divided into 4 groups, namely control group (normal HUVECs), miR-con treatment group, miR-126 mimic treatment group, and miR-126 inhibitor treatment group. In this research, the HUVECs in miR-126 mimic treatment group were transfected with 100 nM of miR-126 mimic using the Lipofectamine 2000 kit (Invitrogen, Carlsbad, CA, USA, lot number: 11573019) strictly according to the experimental operations of the manufacturer's kit. The processing methods in miR-126 inhibitor treatment group were identical to those in miR-126 mimic treatment group except for the concentration of miR-126 inhibitor at 100 nM. After the successful transfection, the cells were cultured in a fresh medium for 24 h and processed with a medium containing oxidized LDL (ox-LDL) for 6 h. Later, the medium containing ox-LDL was sucked, and the cells were washed carefully with aseptic phosphate-buffered saline (PBS) for 3 times, followed by culture in a complete medium for 24 h. The processed cells were used for RT-qPCR, Western blotting, and enzyme-linked immunosorbent assay (ELISA).

In the subsequent investigation, the cells were divided into 4 groups: control group, miR-126 mimic treatment group, miR-126 mimic + sh-S1PR2 treatment group, and miR-126 mimic + sh-con treatment group. S1PR2 was knocked down by shRNA (Qiagen, Cambridge, MA, USA), and the shRNA targeting S1PR2 (30 nM) was transfected into the HUVECs using the Lipofectamine 2000™ transfection reagent (Invitrogen, Carlsbad, CA, USA). 6 h later, the medium containing the transfection reagent was discarded, and the HUVECs were cultured in a fresh medium for another 48 h. After that, the medium containing ox-LDL was added for treatment for 6 h and absorbed. Then, the cells were washed with aseptic PBS for 3 times carefully and cultured with the complete medium for 24 h. The processed cells were used for RT-qPCR, Western blotting, and ELISA.

Luciferase Reporter Assay

The wild-type and mutant-type 3'UTRs of S1PR2 gene were amplified and cloned into psiCHECK™-2 luciferase plasmids (Promega, Madison, WI, USA) to construct the wild-type

Table I. Primer sequences.

Primer name	Primer sequences (5'-3')
MiR-126	5'-CATTATTACTTTTGGTACGC-3' 5'-GAACATGTCTGCGTATCTC-3'
S1PR2	5'-TGGAAACGCAGGAGACGACCTC-3' 5'-CGAGTGGAACTTGCTGTTTCGG-3'
U6	5'-CGCTTCGGCAGCACATATACTA-3' 5'-CGCTTCACGAATTTGCGTGTCA-3'

and mutant-type S1PR2 reporter groups. The primary neurons in mouse spinal cord were cultured in a 24-well plate and co-transfected with miR-126 or miR-con, and wild-type or mutant-type plasmids. The luciferase activity was measured *via* Dual-Luciferase Reporter agent (Promega, Madison, WI, USA) at 48 h after transfection.

Western Blotting Assay

The tissue lysis buffer was prepared, and a proper amount of radioimmunoprecipitation assay (RIPA) and protease inhibitor phenylmethylsulfonyl fluoride (PMSF; RIPA: PMSF=100:1) were added and mixed (Beyotime, Shanghai, China). The cells digested with trypsin were harvested and added with the tissue lysis buffer, and the lysates were collected and transferred into Eppendorf (EP) tubes, followed by centrifugation in a high-speed low-temperature centrifuge at 4°C and 14,000 rpm for 30 min and aspiration of the protein supernatant. Subsequently, the proteins were subjected to a heat bath at 95°C for 10 min for denaturation. The prepared protein samples were stored in a refrigerator at -80°C for later use. The bicinchoninic acid (BCA) kit (Pierce, Rockford, IL, USA) was used to quantify the proteins. After that, the gel for sodium dodecyl sulfate-polyacrylamide gel electrophoresis (SDS-PAGE) was prepared, and the protein samples were loaded into the loading wells of SDS-PAGE for electrophoresis under a constant voltage of 80 V for 2.5 h. Later, the proteins were transferred onto polyvinylidene difluoride (PVDF) membranes (Millipore, Billerica, MA, USA) through semi-dry processes. Subsequently, the PVDF membrane was soaked in Tris-Buffered Saline and Tween-20 (TBST) solution containing 5% skim milk powder and shaken slowly on a table for 1 h for sealing. Next, antibodies were diluted using 5% skim milk powder, and primary antibodies were added for incubation. Then, the membrane was rinsed with TBST solution for 3 times (10 min/time), incubated with secondary antibodies at room temperature for 2 h, and then rinsed with TBST solution twice and TBS once (10 min/time). Subsequently, the proteins were detected using enhanced chemiluminescence (ECL) reagent and exposed in a dark room. Finally, Image-Pro Plus v6 software (Media Cybernetics, Silver Spring, MD, USA) was employed to analyze the relative expression of proteins. The antibodies applied in this research

were all purchased from Abcam (Cambridge, MA, USA).

ELISA

The levels of tumor necrosis factor-alpha (TNF- α), interleukin-1 beta (IL-1 β), and IL-10 secreted by the ox-LDL-treated cells were detected through the ELISA kits according to the manufacturer's instructions.

Animal Experiments

In this research, 60 male apolipoprotein E (ApoE)^{-/-} mice purchased from the Institute of Materia Medica, Peking Union Medical College were divided into 4 groups, namely model group, agomir-126 group, agomir-con group, and antagomir-126 group, using a random number table. The mice in the 4 groups had free access to high-fat diets (21% fat and 0.15% cholesterol) for 15 weeks to establish the CAD model¹⁰. This study was approved by the Animal Ethics Committee of Taihe People's Hospital Animal Center.

Both agomir-126 and antagomir-126 were bought from Shanghai GenePharma Co., Ltd. (Shanghai, China), with the mismatched agomir-126 as the agomir-con in this research. 10 nmol of agomir-126 or 20 nmol of antagomir-126 were dissolved in 0.1 mL of normal saline, and the drugs were injected into the tail vein once every 3 d from the 10th week for 5 weeks.

Hematoxylin and Eosin (HE) Staining

The mice to be examined were killed by dislocation at one time, and the heart was isolated and processed with 4% paraformaldehyde/PBS (pH 7.4) at 4°C for 48 h. After washing with running water, the tissues were dehydrated in 70%, 80%, and 95% ethanol and processed with 100% ethanol, and then the ethanol was eliminated using xylene. Later, the tissues were embedded in paraffin (4 μ m), followed by staining in strict accordance with the manufacturer's instructions of the HE staining kit (Beyotime Biotechnology, Shanghai, China).

Statistical Analysis

All the data were presented as mean \pm SD (standard deviation), the non-paired Student's *t*-test and one-way analysis of variance (ANOVA) were used for statistical analysis between two groups, and Statistical Product and Service Solutions (SPSS) 17.0 (SPSS Inc., Chicago, IL, USA) was employed for statistical analysis in this research.

Results

Differentially Expressed miRNAs in the Serum of CAD Patients Screened Via miRNA Expression Profiles

To explore the differentially expressed miRNAs in the CAD patients, the gene expression profiles in the serum of 3 CAD patients and 3 healthy controls were analyzed. According to the screening results, a total of 211 differentially expressed miRNAs were discovered with $p < 0.05$ as the screening criterion. Next, the results of bioinformatics prediction, with fold change > 5 and $p < 0.01$ as the criteria, further exhibited 43 miRNAs that had potential target genes participating in the pathological process of CAD. Compared with those in control group, 4 miRNAs (miR-126, miR-206, miR-4297, and miR-3646) in the serum of CAD patients displayed the most significant expression differences, which were increased by 6.72, 7.11, 13.57, and 21.22 times, respectively (Figure 1).

Expression Differences in miRNAs Detected Via RT-qPCR Assay

MiRNAs probably exert important effects in the process of coronary atherosclerosis. To further validate the reliability of the high-throughput screening results, 4 markedly up-regulated miRNAs were selected and verified using low-throughput RT-qPCR assay. Results manifested that there were remarkable changes in the expression levels of the 4 selected miRNAs with differential expressions in comparison with those in control group, and the differences were statistically significant ($p < 0.01$). Among them, miR-126 displayed the biggest difference in expression, so it was chosen for subsequent functional verification (Figure 2).

Overexpressed MiR-126 Delayed the Progression of Coronary Atherosclerosis

It was indicated in the HE staining results that there were significantly more coronary atherosclerotic plaques formed in the thoracic aortic region in model group than that in control group. The coronary atherosclerotic plaques were reduced markedly in agomir-126 group, while they were increased prominently in the thoracic aortic region in antagomir-126 group, suggesting that miR-126 may play crucial roles in the pathological process and progression of coronary atherosclerosis (Figure 3A).

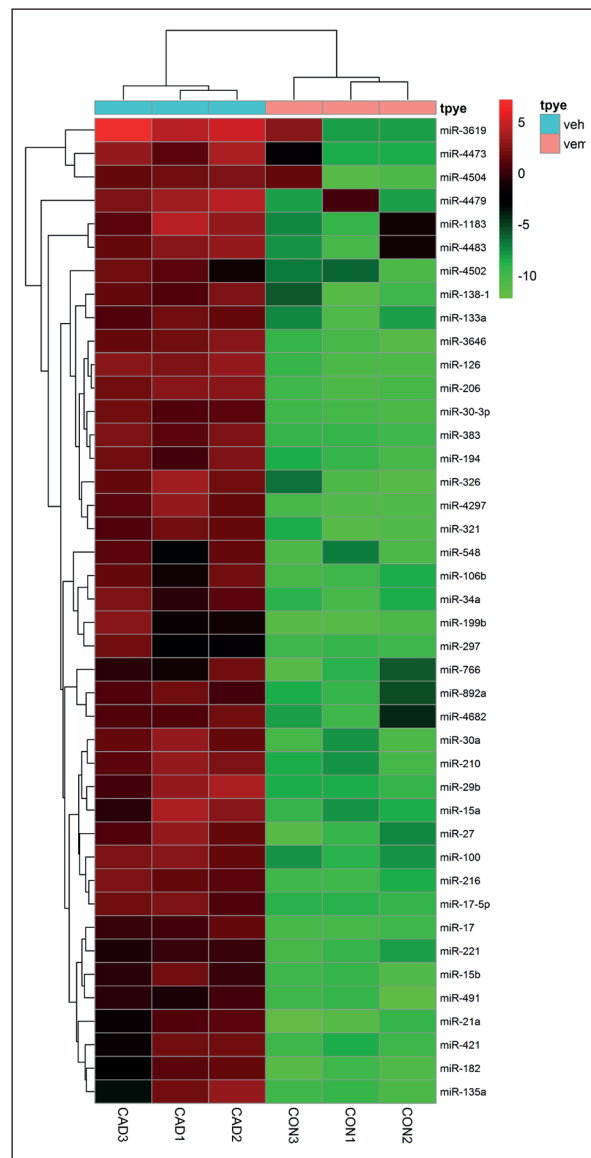


Figure 1. Differentially expressed miRNAs in the serum in CAD group (n=3) and control group (n=3) analyzed via expression profiles. The heat map visualizes the differentially expressed miRNAs with prominent changes (fold change > 5), in which the dark red stands for highly expressed miRNAs, and the bright green for lowly expressed miRNAs.

For the purpose of investigating the influence of miR-126 expression level on the progression of coronary atherosclerosis, agomir-126, and antagomir-126 were utilized to overexpress or knock down the expression of miR-126. It was revealed in RT-qPCR assay results that in comparison with that in agomir-Con group, the expression level of miR-126 was elevated remarkably in the tissues of the thoracic aortic region in agomir-126 group,

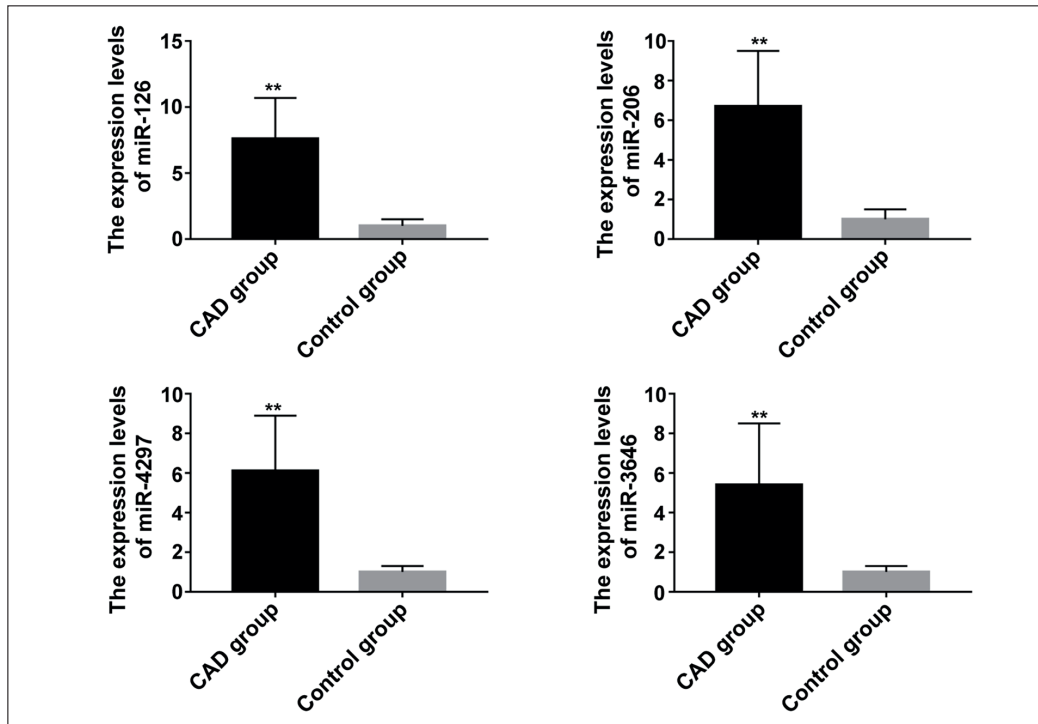


Figure 2. Differences in serum miRNA expressions between CAD group (n=21) and control group (n=30) detected via RT-qPCR assay. The results of RT-qPCR assay manifest that the expression levels of miR-126, miR-206, miR-4297, and miR-3646 in the serum are raised evidently in CAD group compared with those in control group. ** $p < 0.01$.

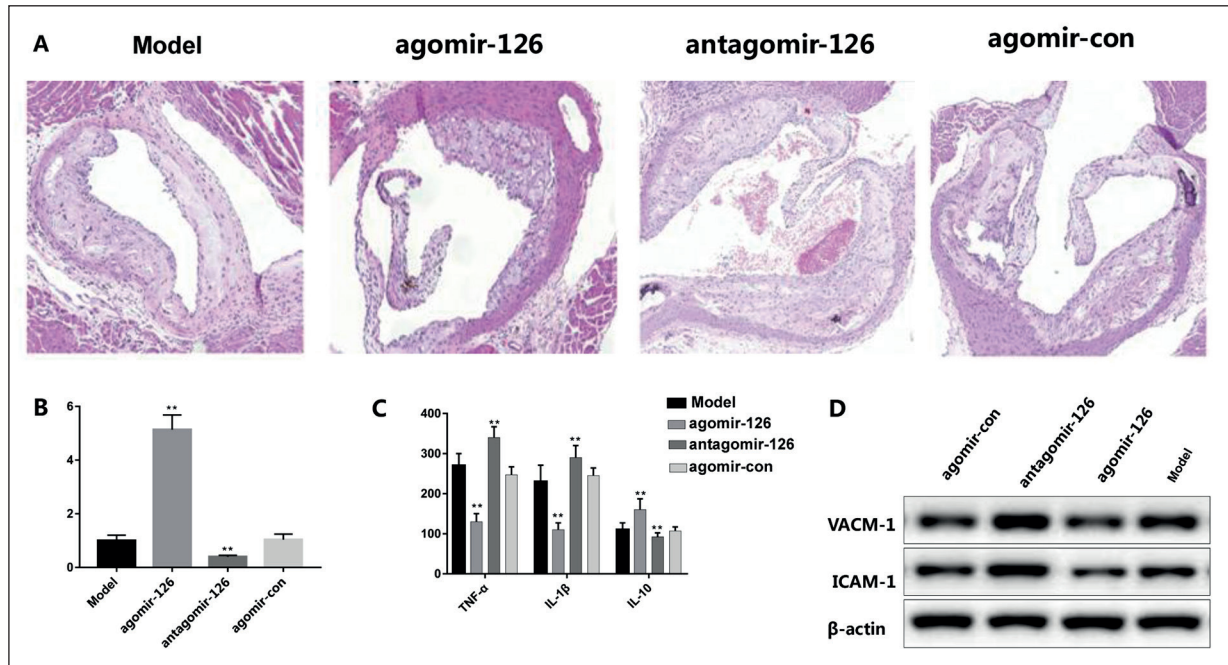


Figure 3. Influences of miR-126 expression level on CAD mouse model. **A**, Influences of different processing methods on tissue morphology in the thoracic aortic region in different groups detected via HE staining (200×). **B**, Influences of different processing methods on serum miR-126 expression level in different groups (n=4) detected via RT-qPCR assay. **C**, Influences of different processing methods on secretion levels of serum TNF- α , IL-1 β , and IL-10 in different groups (n=4) detected via ELISA. **D**, Influences of different processing methods on expression levels of NF- κ B and VACM-1 in tissues of the thoracic aortic region in different groups detected via Western blotting assay.

but it was lowered notably in antagomir-126 group, displaying statistically significant differences ($p < 0.05$; Figure 3B).

To probe the related mechanism of miR-126 in delaying the progression of coronary atherosclerosis, the ELISA results demonstrated that the raised expression level of miR-126 clearly decreased the expressions of serum TNF- α and IL-1 β but significantly increased the expression of IL-10 in the mouse model of CAD. Meanwhile, the lowered expression level of miR-126 distinctly enhanced the expressions of serum TNF- α and IL-1 β but prominently attenuated the expression of IL-10 in the CAD mouse model (Figure 3C). All these data illustrated that the mechanism of miR-126 in delaying the progression of coronary atherosclerosis probably has a correlation with the inflammatory mechanism. The subsequent Western blotting assay further proved the above viewpoints, i.e., the rise in miR-126 expression remarkably reduced the expression levels of nuclear factor-kappa B (NF- κ B) and vascular cell adhesion molecule-1 (VACM-1) in the thoracic aortic region of the CAD mouse model, and vice versa. Besides, there were statistically significant differences in the data ($p < 0.05$) (Figure 3D).

MiR-126 Expression Level was Negatively Correlated with mRNA Expression of S1PR2 in Clinical Samples and CAD Animal Models

The results of analysis through the Pearson correlation coefficient method indicated that the

miR-126 expression level had a negative correlation with S1PR2 expression level in the serum of both CAD patients and animal models ($r = -0.66$, $r = -0.68$) (Figure 4).

MiR-126 Negatively Regulated S1PR2 Expression by Targeting the 3'UTR of S1PR2 mRNA

Through the bioinformatics software, we found that TargetScan S1PR2 might be a potential target of miR-126 (Figure 5A). Then, luciferase reporter assay was adopted to measure the response of wild-type and mutant-type S1PR2 genes in the primary neurons in mouse spinal cord to miR-126 and miR-con to further confirm the interaction between miR-126 and S1PR2 gene. It was discovered that the fluorescence response intensity of HEK293 transfected with miR-126 and wild-type S1PR2 gene declined markedly, while no apparent change in the fluorescence response intensity of HEK293 transfected with mutant-type S1PR2 gene was detected (Figure 5B). In addition, RT-qPCR and Western blotting assays were performed to obtain further evidence. We revealed that the transfection with miR-126 prominently increased the mRNA and protein levels of S1PR2. On the contrary, the knockdown of miR-126 could enhance the expression of S1PR2 gene. In a word, these results elaborated that miR-126 negatively regulates S1PR2 expression by binding to the 3'UTR of S1PR2 mRNA (Figure 5C-E).

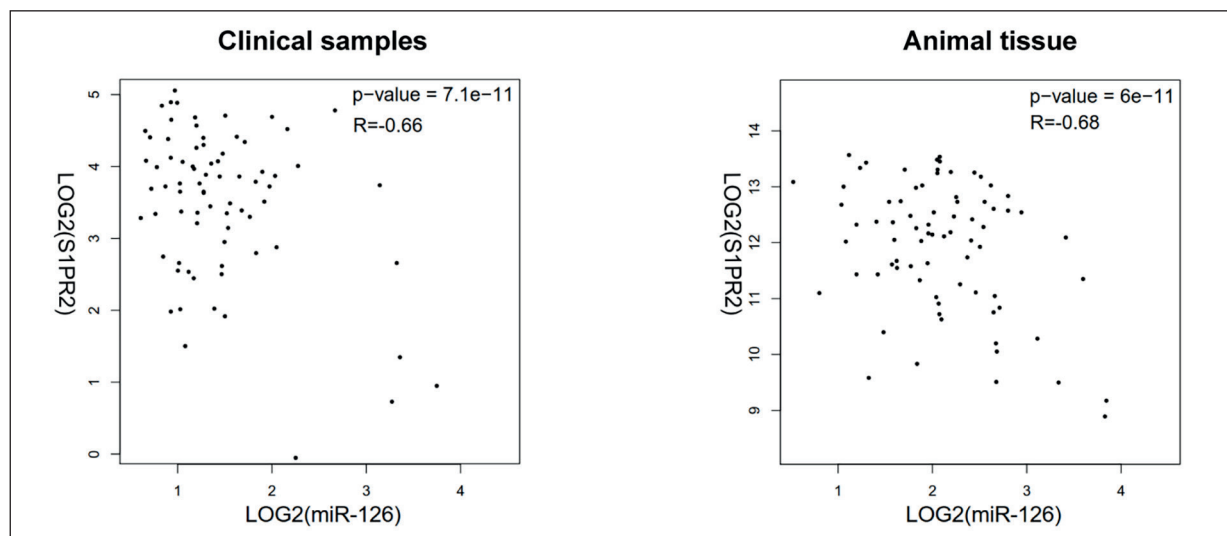


Figure 4. Negative correlation between miR-126 expression level and S1PR2 expression level in clinical samples. The results of Pearson correlation coefficient analysis indicate that the miR-126 expression level has a negative correlation with S1PR2 expression level in the serum of both CAD patients and animal models ($r = -0.6123$, $r = -5.37$).

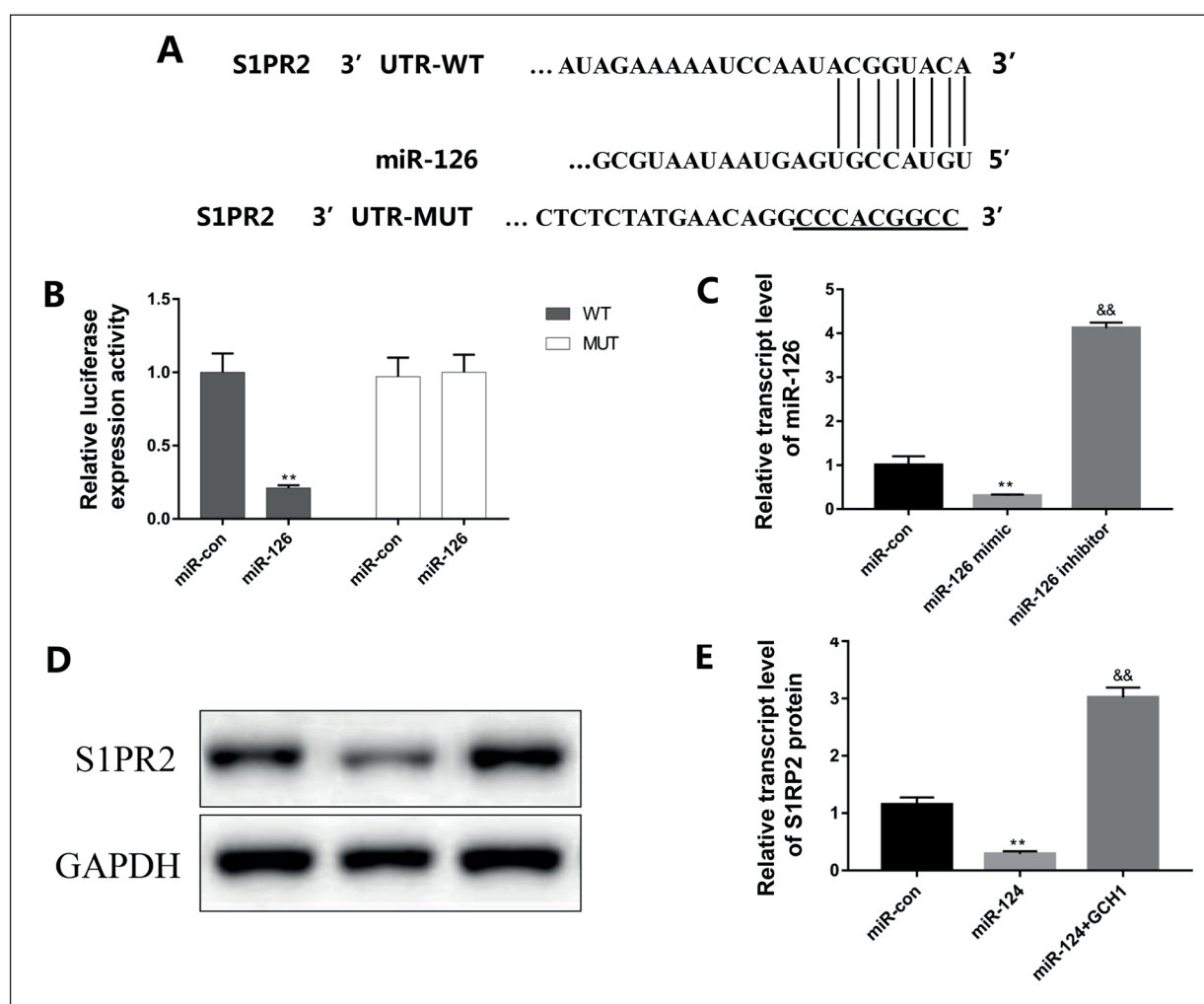


Figure 5. MiR-126 negatively regulates S1PR2 expression by directly binding to the 3'UTR of S1PR2 mRNA. **A**, TargetScan database predicts that miR-126 directly binds to the 3'UTR of S1PR2 mRNA. **B**, Response of wild-type and mutant-type S1PR2 genes in the primary neurons in mouse spinal cord to miR-126 and miR-con detected via luciferase reporter assay. **C**, **D**, **E**, Influences of transfection with miR-con, miR-126, and miR-126 inhibitor on mRNA and protein levels of S1PR2 detected via Western blotting and RT-qPCR assays. **: miR-126 group vs. miR-con group, $p < 0.01$, and &&: miR-126 inhibitor group vs. miR-con group, $p < 0.01$.

Influences of MiR-126 on Expression and Secretion Levels of TNF- α , IL-1 β , and IL-10 in HUVECs

According to the results of Western blotting assay and ELISA, the secretion and expression levels of pro-inflammatory cytokines TNF- α and IL-1 β in HUVECs were significantly elevated, while the expression level of anti-inflammatory cytokine IL-10 declined notably in S1P + ox-LDL (60 $\mu\text{g}/\text{mL}$) treatment group compared with those in S1P (1 μM) treatment group, showing statistically significant differences ($p < 0.01$). Moreover, miR-126 mimic treatment group exhibited markedly lower secretion and

expression levels of pro-inflammatory cytokines TNF- α and IL-1 β , and higher expression level of anti-inflammatory cytokine IL-10 than S1P + ox-LDL (60 $\mu\text{g}/\text{mL}$) treatment group. However, miR-126 inhibitor treatment group had prominently higher secretion and expression levels of pro-inflammatory cytokines TNF- α and IL-1 β , but the lower expression level of anti-inflammatory cytokine IL-10 than S1P + ox-LDL (60 $\mu\text{g}/\text{mL}$) treatment group. All those findings suggest that in the *in vitro* inflammation model, the increased expression level of miR-126 can relieve the inflammation in cells induced by S1P + ox-LDL (Figure 6 A-C).

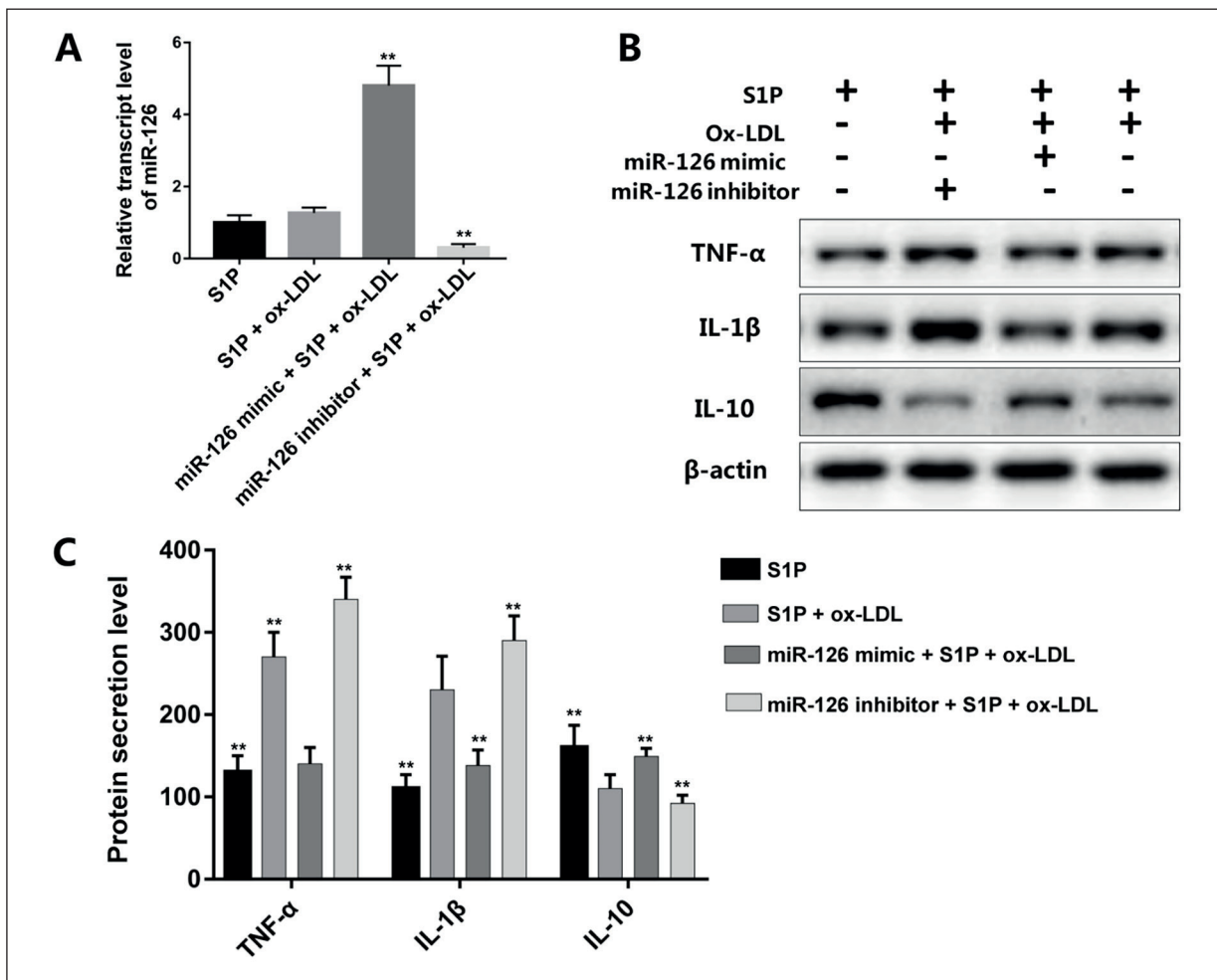


Figure 6. Influences of miR-126 on expression and secretion levels of TNF- α , IL-1 β , and IL-10 in HUVECs. **A**, Expression level of miR-126 in each group of cells detected via RT-qPCR assay. **B**, Influences of miR-126 on secretion levels of inflammatory cytokines TNF- α , IL-1 β , and IL-10 induced by S1P + ox-LDL detected via ELISA. **C**, Influences of miR-126 on expression levels of inflammatory cytokines TNF- α , IL-1 β , and IL-10 induced by S1P + ox-LDL detected via Western blotting assay.

MiR-126 Affected Inflammation Level in HUVECs by Targeting S1PR2

To further explore the influence of miR-126 on the inflammation level in HUVECs induced by S1P + ox-LDL, the lentivirus-shRNA was utilized to knock down the expression level of S1PR2 to determine whether miR-126 affected the elevation in the inflammation level in S1P + ox-LDL-induced HUVECs by targeting S1PR2. The results of RT-qPCR assay manifested that the mRNA and protein expression levels of S1PR2 were decreased evidently in miR-126 mimic treatment group, sh-S1PR2 group, and miR-126 mimic + sh-S1PR2 group in comparison with those in control group. The differences were statistically significant ($p < 0.01$). Nevertheless, there

were no significant differences in the mRNA and protein expression levels of S1PR2 among miR-126 mimic treatment group, sh-S1PR2 group and miR-126 mimic + sh-S1PR2 group. In the results of both Western blotting assay and ELISA we pointed out that the differences in the expression and secretion levels of TNF- α , IL-1 β , and IL-10 were not significant among miR-126 mimic treatment group, sh-S1PR2 group, and miR-126 mimic + sh-S1PR2 group. Additionally, in the results of Western blotting assay we noted that the expression levels of the NF- κ B signaling pathway-related proteins in the cells also displayed no significant differences among the three groups, indicating that miR-126 affects the inflammation level in HUVECs by targeting S1PR2.

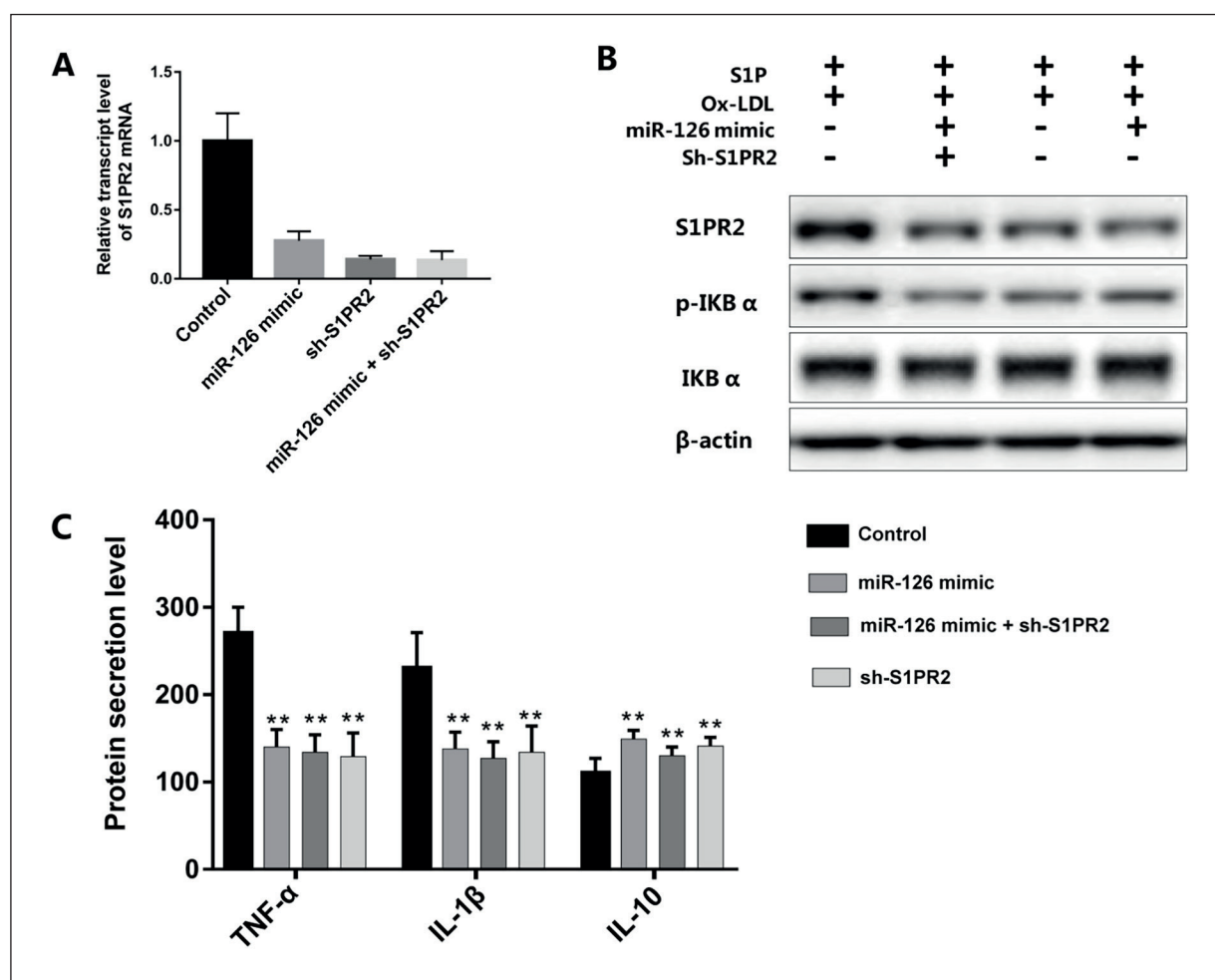


Figure 7. MiR-126 affects inflammation level in HUVECs by targeting S1PR2. **A**, Differences in mRNA expression level of S1PR2 in control group, miR-126 mimic treatment group, sh-S1PR2 group and miR-126 mimic + sh-S1PR2 group detected via RT-qPCR assay. **B**, Differences in expression levels of S1PR2 and NF- κ B signaling pathway in control group, miR-126 mimic treatment group, sh-S1PR2 group, and miR-126 mimic + sh-S1PR2 group detected via Western blotting assay. **C**, Differences in secretion levels of TNF- α , IL-1 β , and IL-10 in control group, miR-126 mimic treatment group, sh-S1PR2 group, and miR-126 mimic + sh-S1PR2 group detected *via* ELISA.

Discussion

CAD is mainly triggered by coronary atherosclerosis, which is a chronic disease accompanied by excessive inflammatory responses and a pathological process involving multiple cell types, including T lymphocytes, macrophages, and endothelial cells¹¹. It is extremely important to diagnose and treat CAD early due to its high morbidity and mortality rates around the world. There is growing evidence that miRNAs are vital players in the pathological process of coronary atherosclerosis, and several studies have demonstrated that miRNAs in the serum can serve as valuable biomarkers for the early diag-

nosis of CAD. For instance, Sullivan et al¹² indicated that the expression levels of miR-15a-5p, miR-16-5p, and miR-93-5p raised distinctly in the serum of CAD patients. Therefore, they can be taken as biomarkers for the early diagnosis of CAD. Although increasingly more miRNAs playing crucial roles in CAD have been discovered so far, there is a limited discussion about their mechanisms of action, thus restricting the clinical application of research findings related to miRNAs.

There were several major results in this research: (1) The expression levels of miR-126, miR-206, miR-4297, and miR-3646 were elevated markedly in the serum of CAD patients, and the

statistical results showed that these 4 miRNAs exhibited the most significant differences, which were further verified by low-throughput RT-qPCR. (2) The results of *in vivo* investigations indicated that the coronary atherosclerotic plaques were reduced remarkably in agomir-126 group, while they were notably increased in the thoracic aortic region in antagomir-126 group. Meanwhile, the elevated expression level of miR-126 evidently lowered the expressions of serum TNF- α and IL-1 β , but significantly increased the expression of IL-10 in the mouse model of CAD. (3) In the bioinformatics prediction and luciferase reporter gene assay we displayed that miR-126 exerted a negative regulatory effect on the S1PR2 expression by targeting the 3'UTR of S1PR2 mRNA. Also, in the analysis results of Pearson correlation coefficient method we manifested that the expression level of miR-126 was negatively correlated with S1PR2 expression level. (4) The increase in miR-126 expression level could reduce the inflammation in S1P + ox-LDL-induced cells in the *in-vitro* inflammation model. (5) The Western blotting assay and ELISA results demonstrated that the differences in the expression and secretion levels of TNF- α , IL-1 β , and IL-10, as well as the expression levels of signaling molecules of the NF- κ B signaling pathway, were not statistically significant among miR-126 mimic treatment group, sh-S1PR2 group, and miR-126 mimic + sh-S1PR2 group, illustrating that miR-126 affects the inflammation level in HUVECs by targeting S1PR2.

In the biological system, S1P is a type of active molecule implicated in lipid regulation, which plays a pivotal role in the cardiovascular system¹³. S1P exerts biological effects by conjugating with its receptors. Currently, a total of 5 kinds of S1PRs have been discovered on the cell surface, and all of them belong to the G protein-coupled receptor family¹⁴. Much attention has been given to the S1P/S1PR2 combination among the 5 S1PRs at present. Increasing reports¹⁵ have pointed out that S1PR2 plays a harmful role in coronary atherosclerosis. In *in vitro* experiments, for example, the S1P/S1PR2 in the cardiomyocytes is able to activate the PKC/NF- κ B signaling pathway, finally stimulating the inflammatory responses¹⁶. The expression levels of inflammatory cytokines such as IL-6, TNF- α , interferon- γ , and MCP-1 are decreased notably in the S1PR2^{-/-} macrophages. Besides, it has been reported that the S1P/S1PR2 can activate the NF- κ B signaling pathway in the endothelial cells, thereby aggravating the

inflammatory responses. The *in vivo* experimental results revealed that the expressions of such pro-inflammatory cytokines as IL-18 and IL-1 β in the serum of S1PR2^{-/-} mice decline prominently, elaborating that S1PR2 exerts an important effect in the inflammatory signals¹⁷. According to the results in this research, miR-126 targeted the 3'UTR of S1PR2 mRNA to negatively regulate the expression of S1PR2. Moreover, no significant differences in the secretion levels of inflammatory cytokines and the activation levels of the NF- κ B signaling pathway were observed between miR-126 mimic treatment group and sh-S1PR2 group, implying that miR-126 influences the inflammation level in HUVECs by targeting S1PR2.

Conclusions

In summary, we revealed that miR-126 is capable of significantly alleviating the progression of CAD and prominently ameliorating the increased inflammation level in HUVECs induced by ox-LDL/S1P, whose action mechanism is associated with the S1PR2 targeting. All these findings elucidate that miR-126 is an important player in the inflammatory process of coronary atherosclerosis, which may become a promising therapeutic target of CAD.

Conflict of Interest

The Authors declare that they have no conflict of interests.

References

- 1) HANSSON GK. Inflammation, atherosclerosis, and coronary artery disease. *N Engl J Med* 2005; 352: 1685-1695.
- 2) NIKPAY M, GOEL A, WON HH, HALL LM, WILLENBORG C, KANONI S, SALEHEEN D, KYRIAKOU T, NELSON CP, HOPEWELL JC, WEBB TR, ZENG L, DEHGHAN A, ALVER M, ARMASU SM, AURO K, BJONNES A, CHASMAN DI, CHEN S, FORD I, FRANCESCHINI N, GIEGER C, GRACE C, GUSTAFSSON S, HUANG J, HWANG SJ, KIM YK, KLEBER ME, LAU KW, LU X, LU Y, LYYTIKAINEN LP, MIHAILOV E, MORRISON AC, PERVIKOV N, QU L, ROSE LM, SALFATI E, SAXENA R, SCHOLZ M, SMITH AV, TIKKANEN E, UITTERLINDEN A, YANG X, ZHANG W, ZHAO W, DE ANDRADE M, DE VRIES PS, VAN ZUYDAM NR, ANAND SS, BERTRAM L, BEUTNER F, DEDOISSIS G, FROSSARD P, GAUGUIER D, GOODALL AH, GOTTESMAN O, HABER M, HAN BG, HUANG J, JALILZADEH S, KESSLER T, KONIG IR, LANNFELT L, LIEB W, LIND L, LINDGREN CM, LOKKI ML, MAGNUSSON PK, MALLICK

- NH, MEHRA N, MEITINGER T, MEMON FU, MORRIS AP, NIEMINEN MS, PEDERSEN NL, PETERS A, RALLIDIS LS, RASHEED A, SAMUEL M, SHAH SH, SINISALO J, STIRRUPS KE, TROMPET S, WANG L, ZAMAN KS, ARDISSINO D, BOERWINKLE E, BORECKI IB, BOTTINGER EP, BURING JE, CHAMBERS JC, COLLINS R, CUPPLES LA, DANESH J, DEMUTH I, ELOSUA R, EPSTEIN SE, ESKO T, FEITOSA MF, FRANCO OH, FRANZOSI MG, GRANGER CB, GU D, GUDNASON V, HALL AS, HAMSTEN A, HARRIS TB, HAZEN SL, HENGSTENBERG C, HOFMAN A, INGELSSON E, IRIBARREN C, JUKEMA JW, KARHUNEN PJ, KIM BJ, KOONER JS, KULLO IJ, LEHTIMAKI T, LOOS R, MELANDER O, METSPALU A, MARZ W, PALMER CN, PEROLA M, QUERTERMOUS T, RADER DJ, RIDKER PM, RIPATTI S, ROBERTS R, SALOMAA V, SANGHERA DK, SCHWARTZ SM, SEENDORF U, STEWART AF, STOTT DJ, THIERY J, ZALLOUA PA, O'DONNELL CJ, REILLY MP, ASSIMES TL, THOMPSON JR, ERDMANN J, CLARKE R, WATKINS H, KATHIRESAN S, MCPHERSON R, DELOUKAS P, SCHUNKERT H, SAMANI NJ, FARRALL M. A comprehensive 1,000 genomes-based genome-wide association meta-analysis of coronary artery disease. *Nat Genet* 2015; 47: 1121-1130.
- 3) HOWSON J, ZHAO W, BARNES DR, HO WK, YOUNG R, PAUL DS, WAITE LL, FREITAG DF, FAUMAN EB, SALFATI EL, SUN BB, EICHER JD, JOHNSON AD, SHEU W, NIELSEN SF, LIN WY, SURENDRAN P, MALARSTIG A, WILK JB, TYBJAERG-HANSEN A, RASMUSSEN KL, KAMSTRUP PR, DELOUKAS P, ERDMANN J, KATHIRESAN S, SAMANI NJ, SCHUNKERT H, WATKINS H, DO R, RADER DJ, JOHNSON JA, HAZEN SL, QUYYUMI AA, SPERTUS JA, PEPINE CJ, FRANCESCHINI N, JUSTICE A, REINER AP, BUYSKE S, HINDORFF LA, CARTY CL, NORTH KE, KOOPERBERG C, BOERWINKLE E, YOUNG K, GRAFF M, PETERS U, ABSHER D, HSIUNG CA, LEE WJ, TAYLOR KD, CHEN YH, LEE IT, GUO X, CHUNG RH, HUNG YJ, ROTTER JI, JUANG JJ, QUERTERMOUS T, WANG TD, RASHEED A, FROSSARD P, ALAM DS, MAJUMDER A, DI ANGELANTONIO E, CHOWDHURY R, CHEN YI, NORDESTGAARD BG, ASSIMES TL, DANESH J, BUTTERWORTH AS, SALEHEEN D. Fifteen new risk loci for coronary artery disease highlight arterial-wall-specific mechanisms. *Nat Genet* 2017; 49: 1113-1119.
 - 4) SHIRAI T, NAZAREWICZ RR, WALLIS BB, YANES RE, WATANABE R, HILHORST M, TIAN L, HARRISON DG, GIACOMINI JC, ASSIMES TL, GORONZY JJ, WEYAND CM. The glycolytic enzyme PKM2 bridges metabolic and inflammatory dysfunction in coronary artery disease. *J Exp Med* 2016; 213: 337-354.
 - 5) KARAKAS M, SCHULTE C, APPELBAUM S, OJEDA F, LACKNER KJ, MUNZEL T, SCHNABEL RB, BLANKENBERG S, ZELLER T. Circulating microRNAs strongly predict cardiovascular death in patients with coronary artery disease-results from the large AtheroGene study. *Eur Heart J* 2017; 38: 516-523.
 - 6) MIRZAEI H, FERNS GA, AVAN A, MOBARHAN MG. Cytokines and microRNA in coronary artery disease. *Adv Clin Chem* 2017; 82: 47-70.
 - 7) ECONOMOU EK, OIKONOMOU E, SIASOS G, PAPAGEORGIOU N, TSALAMANDRIS S, MOUROUZIS K, PAPAIOANOU S, TOUSOULIS D. The role of microRNAs in coronary artery disease: from pathophysiology to diagnosis and treatment. *Atherosclerosis* 2015; 241: 624-633.
 - 8) SCHULTE C, MOLZ S, APPELBAUM S, KARAKAS M, OJEDA F, LAU DM, HARTMANN T, LACKNER KJ, WESTERMANN D, SCHNABEL RB, BLANKENBERG S, ZELLER T. MiRNA-197 and miRNA-223 predict cardiovascular death in a cohort of patients with symptomatic coronary artery disease. *PLoS One* 2015; 10: e145930.
 - 9) WIDMER RJ, LERMAN LO, LERMAN A. MicroRNAs: small molecule, big potential for coronary artery disease. *Eur Heart J* 2016; 37: 1750-1752.
 - 10) CAMACHO P, FAN H, LIU Z, HE JO. Small mammalian animal models of heart disease. *Am J Cardiovasc Dis* 2016; 6: 70-80.
 - 11) BOULANGER CM, LOYER X, RAUTOU PE, AMABILE N. Extracellular vesicles in coronary artery disease. *Nat Rev Cardiol* 2017; 14: 259-272.
 - 12) O SULLIVAN JF, NEYLON A, MCGORRIAN C, BLAKE GJ. MiRNA-93-5p and other miRNAs as predictors of coronary artery disease and STEMI. *Int J Cardiol* 2016; 224: 310-316.
 - 13) YAMADA Y, WAKAO S, KUSHIDA Y, MINATOGUCHI S, MIKAMI A, HIGASHI K, BABA S, SHIGEMOTO T, KURODA Y, KANAMORI H, AMIN M, KAWASAKI M, NISHIGAKI K, TAOKA M, ISOBE T, MURAMATSU C, DEZAWA M, MINATOGUCHI S. S1P-S1PR2 axis mediates homing of muse cells into damaged heart for long-lasting tissue repair and functional recovery after acute myocardial infarction. *Circ Res* 2018; 122: 1069-1083.
 - 14) LEVKAU B. HDL-S1P: cardiovascular functions, disease-associated alterations, and therapeutic applications. *Front Pharmacol* 2015; 6: 243.
 - 15) MARTIN R, SOSPEDRA M. Sphingosine-1 phosphate and central nervous system. *Curr Top Microbiol Immunol* 2014; 378: 149-170.
 - 16) REN K, LU YJ, MO ZC, LIU X, TANG ZL, JIANG Y, PENG XS, LI L, ZHANG OH, YI GH. ApoA-I/SR-BI modulates S1P/S1PR2-mediated inflammation through the PI3K/Akt signaling pathway in HUVECs. *J Physiol Biochem* 2017; 73: 287-296.
 - 17) ZHANG G, YANG L, KIM GS, RYAN K, LU S, O'DONNELL RK, SPOKES K, SHAPIRO N, AIRD WC, KLUK MJ, YANO K, SANCHEZ T. Critical role of sphingosine-1-phosphate receptor 2 (S1PR2) in acute vascular inflammation. *Blood* 2013; 122: 443-455.